Anatomy and efficiency of urban multimodal mobility

Riccardo Gallotti* and Marc Barthelemy†
Institut de Physique Théorique, CEA, CNRS-URA 2306, F-91191, Gif-sur-Yvette, France

SUPPLEMENTARY INFORMATION

Data Filtering and Elaboration

Not all Stop Points are actually used, so only those that were present in the timetables are considered active and have been taken into account. Stop points are then organized into Stop Areas representing facilities (Airports, Bus/Metro/Coach/Railway Stations) or possible interchange points. The definition of these Stop areas has been taken as a basis for defining a multi-layer network form the timetable data. A further process of data cleaning and aggregation has been performed to have a consistent definition of inter-modal exchange points.

Inconsistent stop times have been corrected by temporal interpolation whenever possible. In the other cases, the stop has been excluded from the dataset. In particular: i) Many inconsistencies were found in bus stop times: they have been considered wrong whenever two following stops happened more than 2 hours one from another (this applies also the case of decreasing times) ii) In the original rail timetables, many stop time were erroneously recorded as '0000': temporal interpolation solved this problem almost entirely.

Inconsistent NaPTAN Stop Areas have been corrected, using as a reference parameter a Walking Distance $wd =$ 500m. The procedure follow those steps:

i) the Center of an Area, identified by Latitude and Longitude, are corrected with the Stop Points center of mass if before the corrections not all Points were within a distance wd from the Center and after they were;

ii) Points where Air, Ferry, Rail, Metro and Coach stops happen are always kept in the Area, Bus stops Points further than wd from the Center are removed;

iii) Areas containing only Bus stops Points are corrected by removing the further stops (and recalculating the center of mass) until they become contained in a circular area of radius $wd/2$ (thus a maximal distance between two points of wd);

iv) Airports Stop Points and Areas are joined together if they share the same first 6 letters in atcocode;

v) All Air Stop Points are "promoted" to Areas;

vi) The Heathrow Airport stop Area is reconstructed "by hand" as the Stop Area was incorrectly defined;

vii) After imposing a hierarchy $[A > F > R > M > C > B]$, all Areas include other Areas and non-bus stops Points of lower rank within a distance wd from its Center (distance between Areas is defined as the distance between their center);

viii) All remaining non-bus stops Points are "promoted" to Areas;

ix) Rail ,Metro and Ferry Areas of same rank are merged if their distance were under wd (Rail) or $wd/2$ (Ferry,Metro). The choice of $wd/2$ is to avoid joining together following Stops of London Tub and Ferries lines;

x) All Areas can absorb a Bus stop Point if it is within a distance $wd/2$. In case of conflict, the Point is assigned to the closest;

xi) Areas containing only one Point are "declassed" to Points;

xii) A stop Point can absorb lower rank Areas/Points if it is within a distance $wd/2$ and become an Area (C and B Points cannot absorb in this step);

xiii) To each Area is assigned a representing Point, chosen at random between those with higher rank.

The so-defined Areas become the inter-layer point for the Multi-layer network. The distance assigned as a inter-layer weight is then computed as the average distance between all Points of the first layer and all Points of the second layer.

A copy of this dataset is publicly available at http://www.quanturb.com/data.html

Cities

In this paper, we identify as a city a circular area roughly containing the borders of the associated urban area. Each circle is defined by the latitude and the longitude of its center and by its radius (see table below). The value of the population for the relative Morphological Urban Areas, obtained from wikipedia.org [http://en.wikipedia.org/wiki/List_of_metropolitan_areas_in_the_United_Kingdom (Date of access:06/05/2014)] is associated to each of these areas. For London, two different areas have been studied. The first one is larger and corresponds to the whole Greater London, while a second, smaller, only the group of inner boroughs commonly named Inner London [http://en.wikipedia.org/wiki/Inner_London (Date of access:06/05/2014)]. Due to our rough selection of the urban area surface, the value of population used is to be considered only an approximation of the real population of the selected surface.

City Name	Lat	Lon	Radius (km)	Population	Ω (trips/hour)
Greater London	51.51	-0.12	28	8,265,000	196,594
Inner London	51.51	-0.12	14	3,232,000	120,937
Manchester	53.48	-2.24	18	2,207,000	51,974
Birmingham	52.48	-1.89	18	2,363,000	61,225
Glasgow	55.86	-4.26	15	1.228,000	35,446
Leeds	53.80	-1.55	10	534,000	15,158
Liverpool	53.40	-2.98	13	1.170,000	26,444
Bristol	51.45	-2.58	12	568,000	9,583
Sheffield	53.38	-1.42	12	693,000	26,243
Edinburgh	55.95	-3.18	10	478,000	37,942
Cardiff	51.48	-3.18	8	353,000	6685

Not all transportation modes are available in every city. Naturally, air transport is not playing any role and the water transport is available only in London, Liverpool and Bristol. Moreover, the mode of transport associated to the Metro layer may be different from a city to another. In London two types of transportation networks can be associated to the M-layer: the Underground and Tram. A circular line of Subways is available also in Glasgow, while in Manchester, Birmingham and Sheffield the Metro Layer represents the Tram network. In the other cities considered here, there are no Metro layer.

Detour

In both time-respecting paths (figure 1 Left) and minimal paths, the detour $r(d) = \ell(d)/d$, where ℓ is the effective path's length and d the euclidean distance between origin and destination, is a decreasing function of d. In our analysis, we exclude trips where origin and destination are less than 1 km apart, and the quantity $R = \max_{d>1} r(d)$ corresponds in our case to the detour for the shortest considered path $r(1km)$. In figure 1 Right, we see that R decreases when the average cyclomatic number $M_N = (E - N - 1)/N$ grows, where E is the number of directed edges and N the number of nodes of the network. This suggests that the availability of more alternatives, characterized by a larger number of cycles per node in the network, makes straighter trajectories possible.

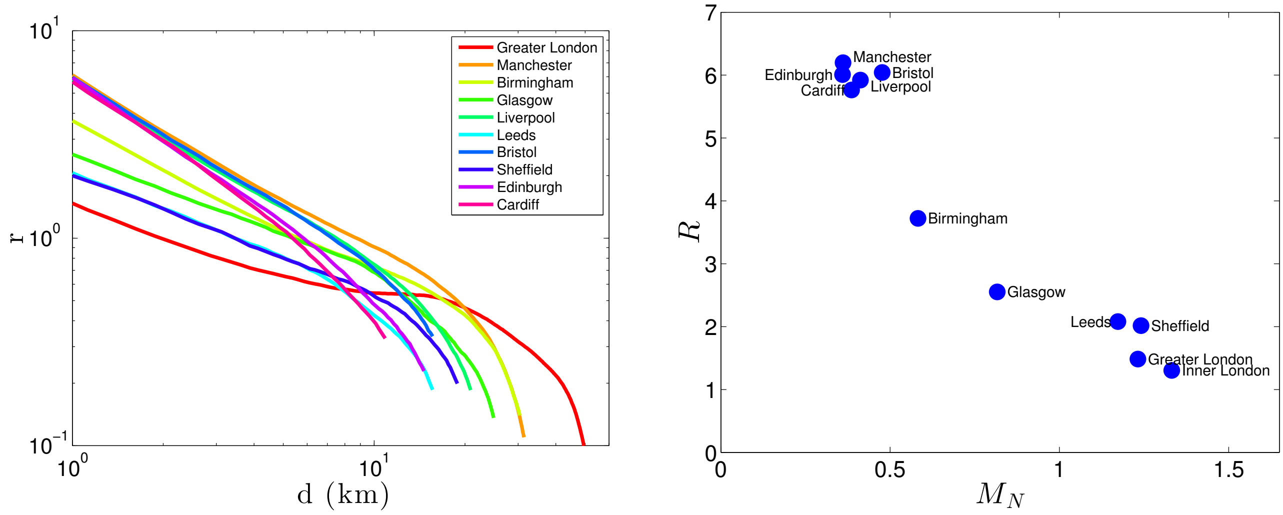

FIG. 1: (Left) Detour Profiles $r(d)$ in different urban areas. (Right) The peak value (R) of the detour profiles, decreasing with the average cyclomatic number M_N.

Connection times in multi-modal trajectories

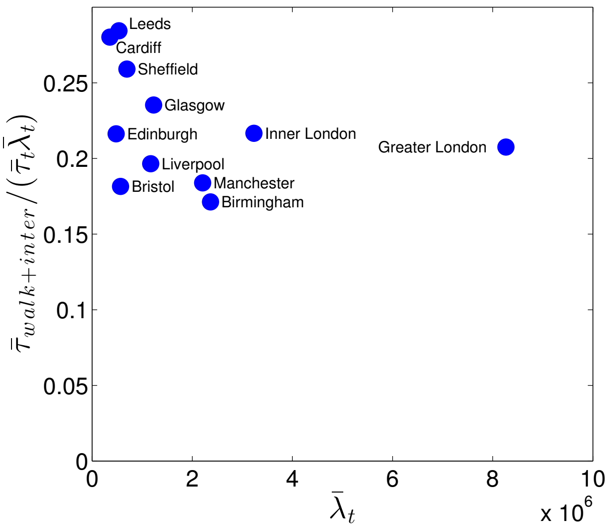

FIG. 2: **The average inter-layer connection time for a city, defined as the sum of the walking time and the inter-layer waiting time $\bar{\tau}_{walk+inter}$ over the total traveltime $\bar{\tau}$ clearly depends upon the fraction $\bar{\lambda}_t$ of trajectories that have inter-layer connections. Dividing by $\bar{\lambda}_t$, we estimate the average fraction of inter-layer connection time, restricted to the interdependent trajectories. We notice that, for cities of different size and offer for transport service, this value is relatively stable and all values can be found in the interval $23\% \pm 6\%$.**

Time-respecting Paths Travel Speeds

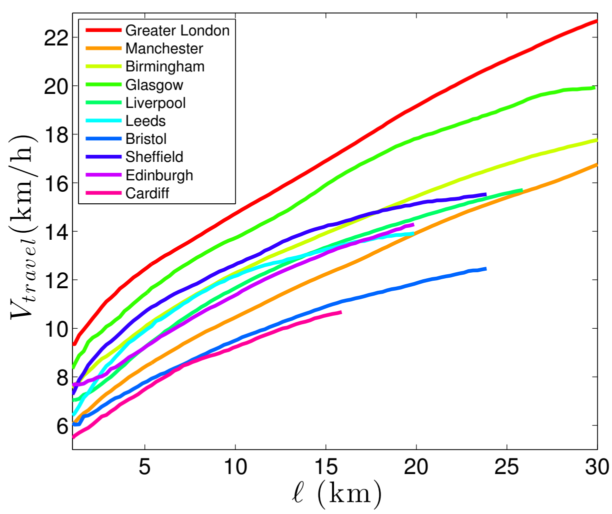

FIG. 3: The travel speed $V_{travel} = \ell/\tau_t$ grows with the trip's length ℓ and seem not to reach any saturation value within the urban areas' radios. In the main paper, we show that the average value $\bar{V}_{travel}$ is linked to the interdependency λ and, as a consequence, to the average number of stop events per hour Ω or to the urban area population.

Average speeds and frequencies

Let $e_k^\alpha = (i, j)$ be a directed edge from a vertex i to a second vertex j, both belonging to layer α. The edge is identified by the index $k = 1 \dots E_\alpha$. Each edge is characterized a the speed $V(e_k^\alpha)$ and the frequency $f(e_k^\alpha) = C(e_k^\alpha)/\Delta t$, where $C(e_k^\alpha)$ is the number of departure events through the edge e_k^α in the time interval Δt. As our study is focussed on the mobility starting at 8:00 of a working Monday, we chose as extremes of the time interval $t_{end} =$ 24:00 $t_0 =$ 08:00 of Monday, and thus $\Delta t = 16$h.

For every city, we may define the average speed of a layer α as the average over all edges's speed for that layer:

$$\bar{V}_\alpha = \sum_{k=1}^{E_\alpha} V(e_k^\alpha)/E_\alpha \tag{1}$$

and, similarly, the average frequency is:

$$\bar{f}_\alpha = \sum_{k=1}^{E_\alpha} f(e_k^\alpha)/E_\alpha \tag{2}$$

In figures and we see how these quantities differ significantly between the considered cities.

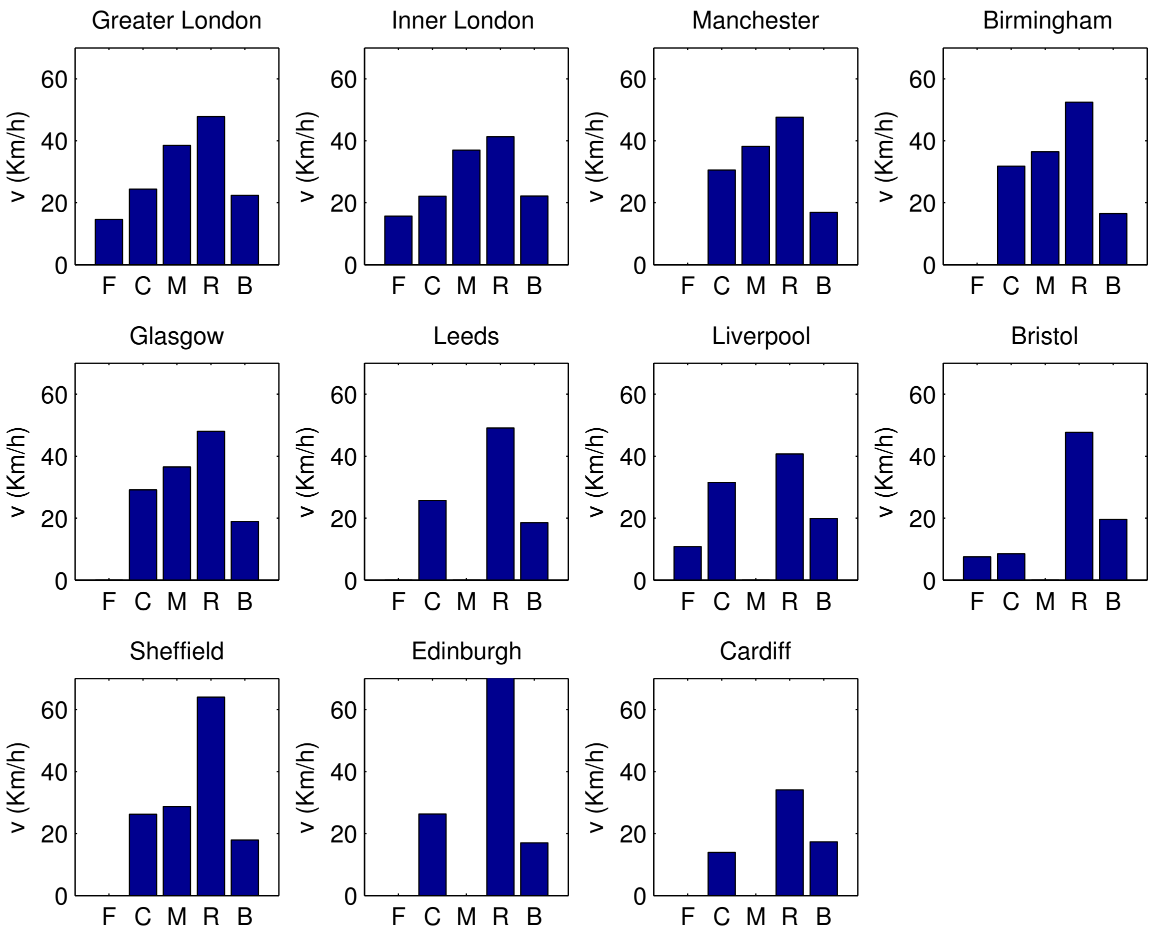

FIG. 4: Average layer edges' speed V_α in the different Public Transport Networks: F=Ferry, C=Coach, M-Metro, R=Rail, B=Bus. Note that the Ferry and Metro layer are not available in all cities.

In our time-respecting paths, only the Bus, Rail and, when available, Metro layer play a major role. To compare the results of cities where the Metro layer is available with cities where it is not, we introduce the average non-bus speed $\bar{V}_{nb}$ and frequency $\bar{f}_{nb}$ defined as:

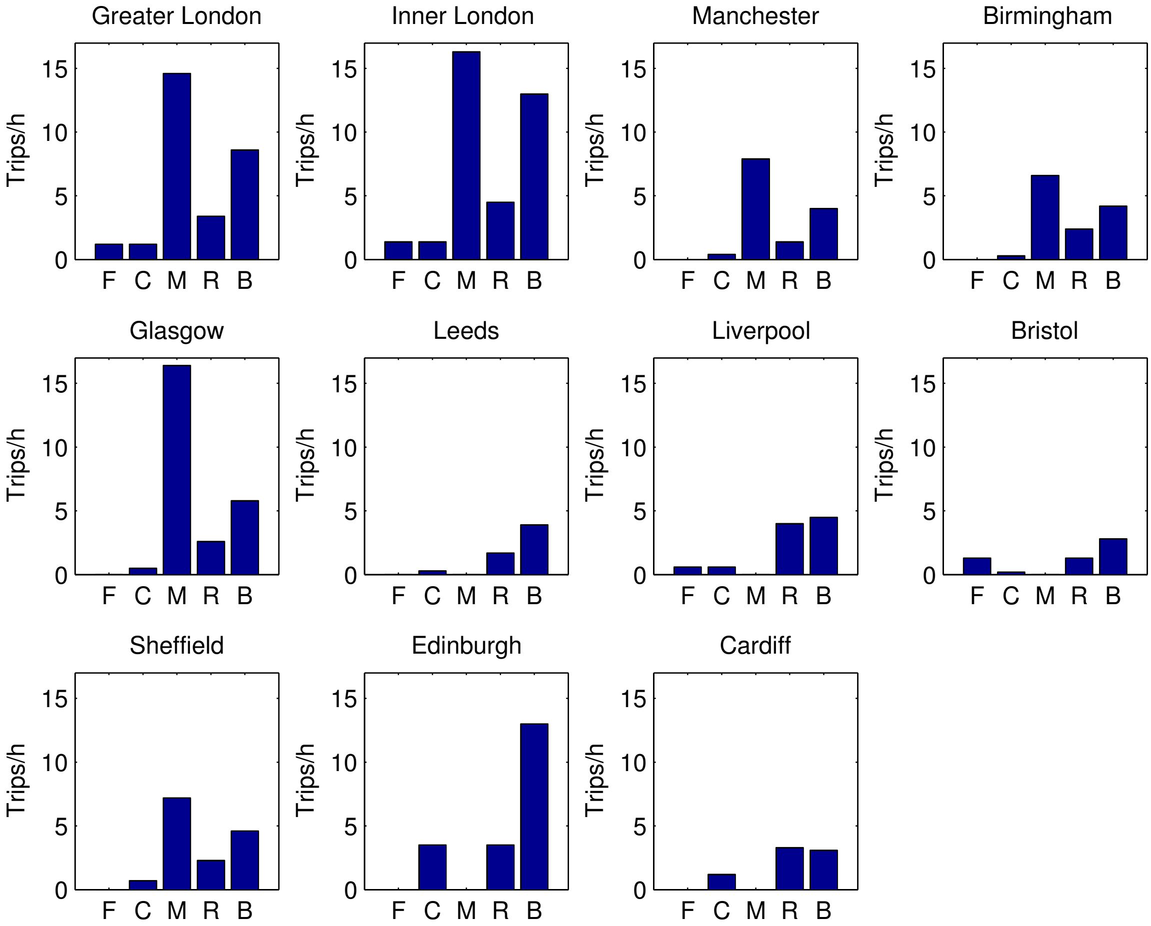

FIG. 5: Average layer edges' frequencies f_α in the different Public Transport Networks: F=Ferry, C=Coach, M-Metro, R=Rail, B=Bus. Note that the Ferry and Metro layer are not available in all cities.

$$\bar{V}_{nb} = \frac{\bar{\ell}_m}{\bar{\ell}} V_m + \frac{\bar{\ell}_r}{\bar{\ell}} V_r \tag{3}$$

and the average frequency:

$$\bar{f}_{nb} = \frac{\bar{\ell}_m}{\bar{\ell}} f_m + \frac{\bar{\ell}_r}{\bar{\ell}} f_r \tag{4}$$

where $\frac{\bar{\ell}_m}{\ell}$ and $\frac{\bar{\ell}_r}{\ell}$ are, for each city, the average on all trips of the fraction of the total length ℓ that is covered on the Metro (m) or Rail (r) layer respectively. As we see in figure 6, this simple proportion permits us to reconstruct reasonably well the differences of cruise speed $V_{cruise} = \langle \ell / \tau_r ide \rangle$ in different cities.

Average interdependency and speed

Hypothesis: the number of possible alternative to exclusive bus layer path (which is always an available option) is $\propto \Omega$. Thus, fraction of paths using only the bus layer is

$$1 - \lambda_t = \frac{1}{1 + a_\lambda \Omega}$$

and conversely

$$\lambda_t = \frac{a_\lambda \Omega}{1 + a_\lambda \Omega}$$

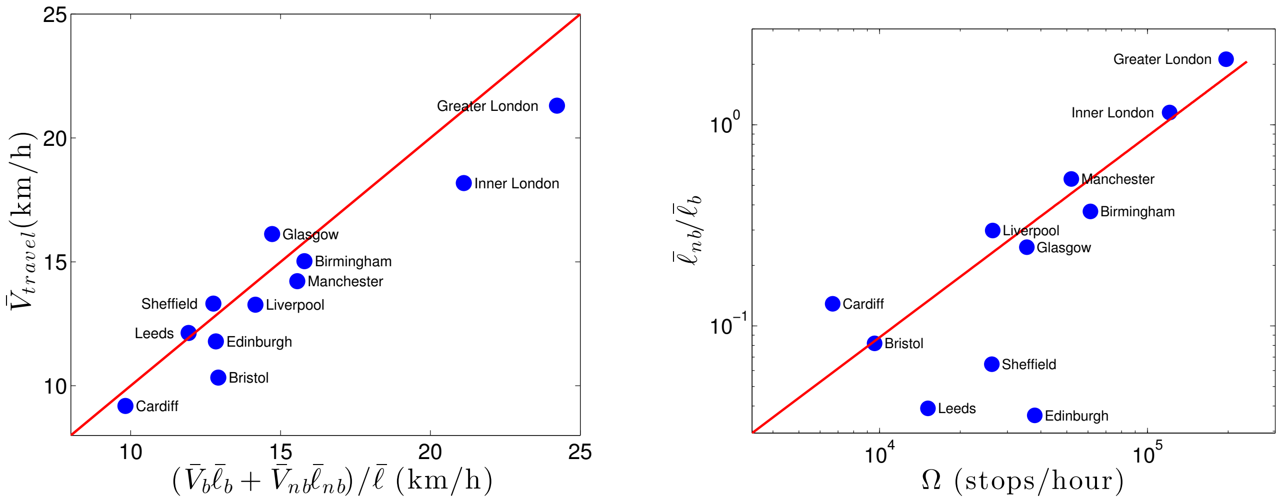

FIG. 6: (Left) The average cruise speeds can be estimated by knowing for each layer: i) the average link's speeds; ii) the fraction of length covered in that layer. (RIght) The ratio $\bar{f}_{nb}/\bar{f}_b$ grows with Ω. The solid line is a guide for the eye suggesting a direct proportion.

Hypothesis: once the non-bus layers are involved, there is a proportion between the distance covered in the bus ℓ_b ant the distance covered in the non-bus $\ell_n b$

$$k = \frac{\ell_{nb}}{\ell_b}$$

With this assumption, V_{cruise} reads

$$V_{cruise} = V_b(1-\lambda_t) + \frac{V_b\ell_b + V_{nb}\ell_{nb}}{\ell_b + \ell_{nb}}\lambda_t$$
$$= \frac{V_b + \frac{\frac{V_b}{V_{nb}}+k}{1+k}V_{nb}a_\lambda\Omega}{1+a_\lambda\Omega}$$

Contributions to the inefficiency

In our paper, we show that the average synchronization inefficiency $\delta = \tau_t/\tau_m - 1$ decreases when Ω grows. More specifically, there are two factors contributing to a lower inefficiency: cruise speeds in the time-respecting paths become progressively closer to those of minimal paths (fig. 7 Left), and a lower relative contribution of the waiting times (inter- and intra-layer) to the total travel time (fig. 7 Right).

Walking time and Multi-modality

Anatomies

Here below we complete the overview of the Anatomy of the transport networks described in figure 6 of the Paper.

* Electronic address: rgallotti@gmail.com
† Electronic address: marc.barthelemy@cea.fr

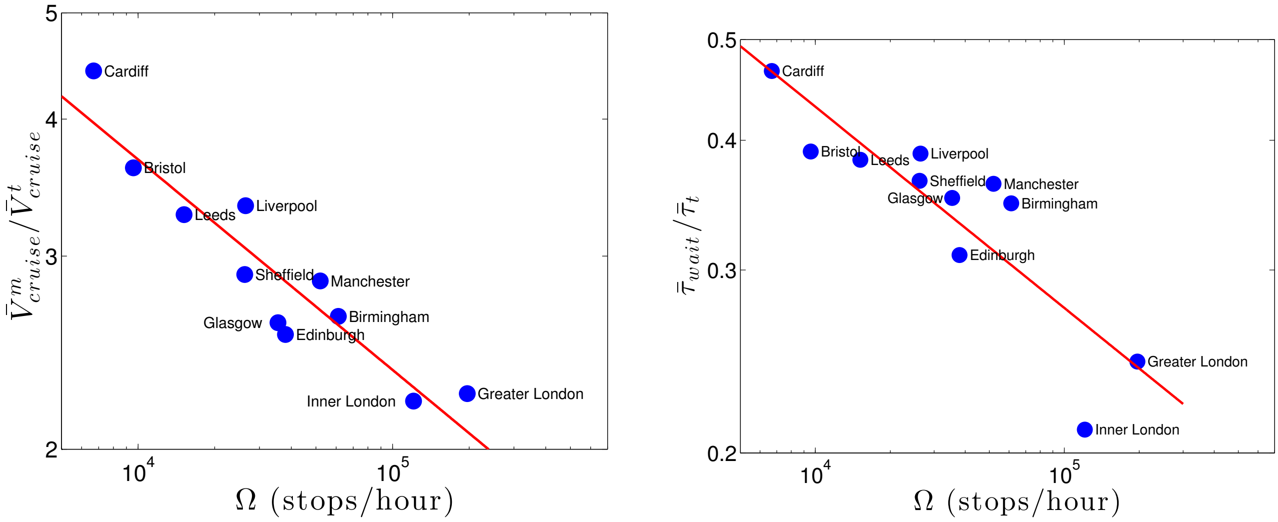

FIG. 7: (Left) The ratio between the average cruise speed in time-respecting paths V^t_{cruise} and in minimal pathsV^m_{cruise} falls with Ω as $V^t_{cruise}/V^m_{cruise} \propto \Omega^{-0.19\pm0.06}$ ($R^2 = 0.87$). (Right) The relative weight of waiting times τ_{wait} over the total travel times τ_t for time-respecting paths decreases also as $\tau_{wait}/\tau_t \propto \Omega^{-0.19\pm0.08}$ ($R^2 = 0.76$).

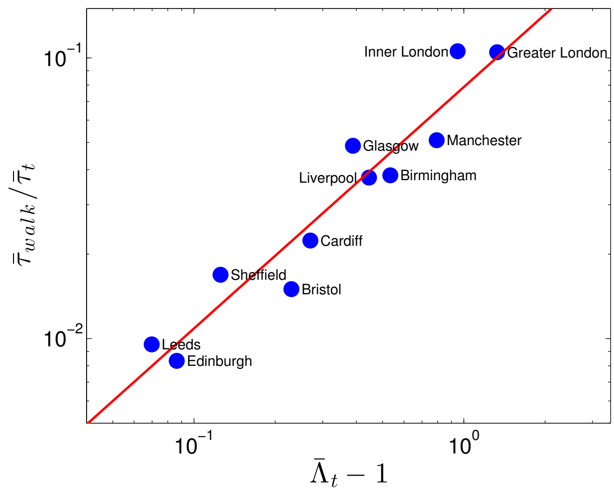

FIG. 8: As one may expect, the fraction of travel time spent walking grows with the average number $\bar{\Lambda}_t$ of layers (and thus of connections) involved in the time-respecting paths. The growth is consistent with a direct proportionality: $\tau_{walk}/\tau_t \propto \Lambda^{-0.9\pm0.2}$ ($R^2 = 0.92$)

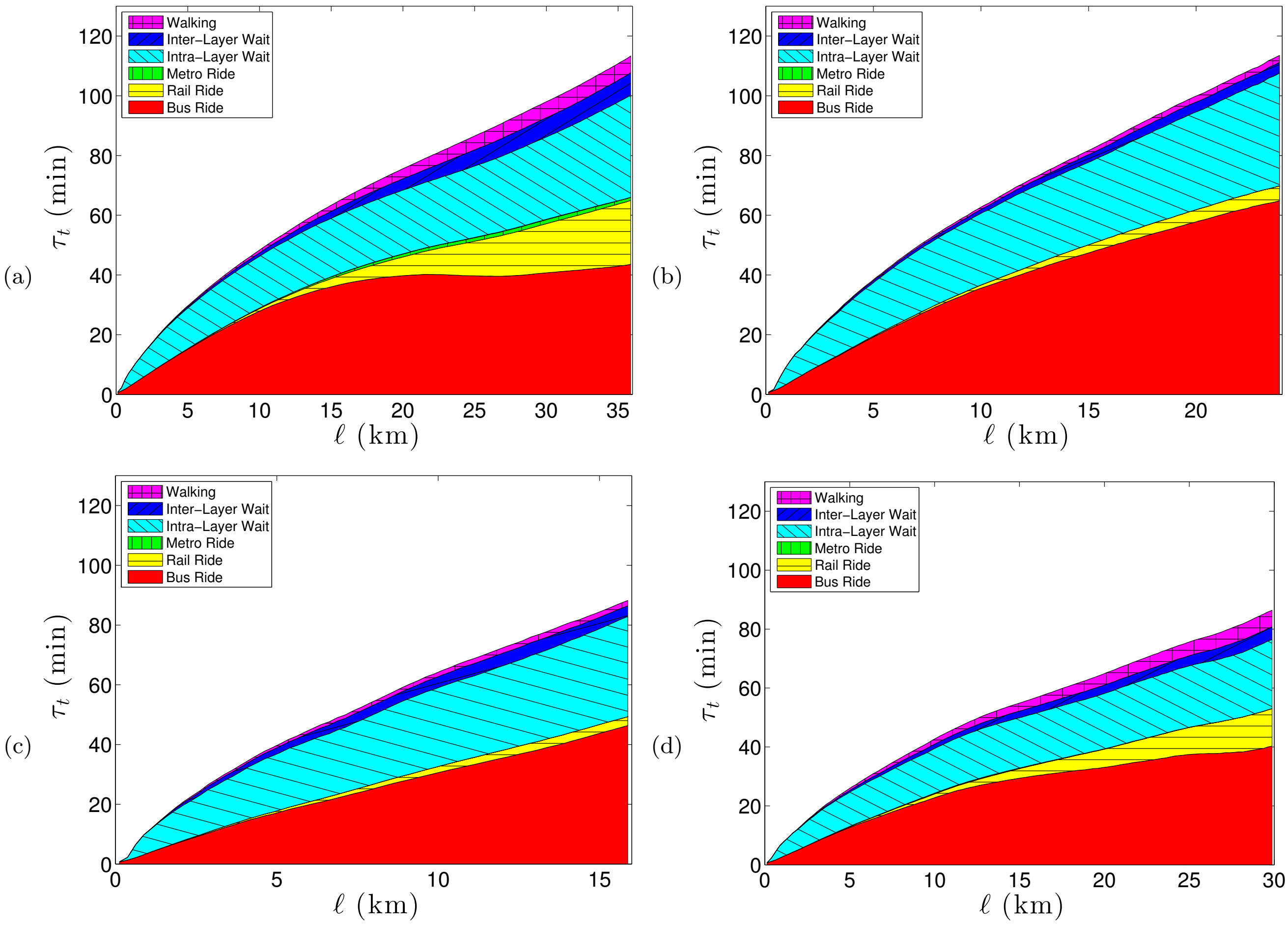

FIG. 9: The Anatomy of the transport networks in: (a) Birmingham; (b) Bristol; (c) Cardiff; (d) Glasgow

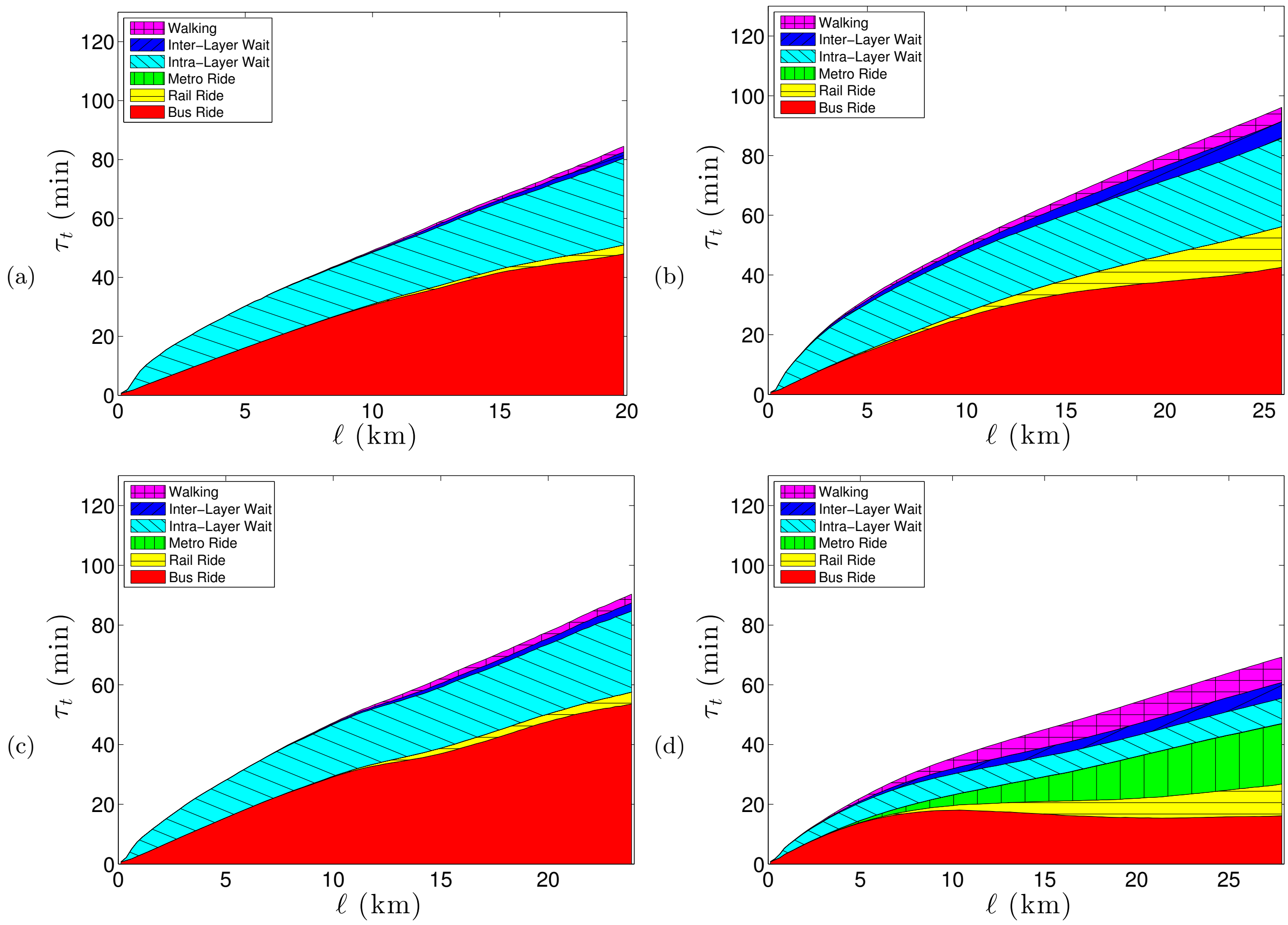

FIG. 10: The Anatomy of the transport networks in: (a) Leeds; (b) Liverpool; (c) Sheffield; (d) Inner London